TransDetect identifies a new regulatory module controlling phosphate accumulation.

Sikander Pal, Mushtak Kisko, Christian Dubos, Benoît Lacombe, Pierre Berthomieu, Gabriel Krouk, Hatem Rouached

Plant Physiology Preview. Published on August 21, 2017, as DOI:10.1104/pp.17.00568

TransDetect identifies a new regulatory module controlling phosphate accumulation

Sikander Pal[¶], Mushtak Kisko[¶], Christian Dubos, Benoit Lacombe, Pierre Berthomieu, Gabriel Krouk*, Hatem Rouached*[,§]

Laboratoire de Biochimie & Physiologie Moléculaire des Plantes, UMR CNRS/INRA/Montpellier Supagro/UM, Institut de Biologie Intégrative des Plantes 'Claude Grignon', 2 Place Pierre Viala, 34060 Montpellier, France.

[§]Present address: Department of Plant Biology, Carnegie Institution for Science, 260 Panama Street, Stanford, CA 94305, USA.

*To whom correspondence should be addressed:

Dr Hatem ROUACHED (hatem.rouached@inra.fr)

Dr Gabriel KROUK (gkrouk@gmail.com)

BPMP. BAT7- 2 Place Pierre Viala. 34060 Montpellier Cedex FRANCE

Fax : +33 (0) 4 67 52 57 37

[¶]Authors equally contributed to this work

Funding information. The TransDetect algorithm development was supported by the Laboratoire International Associé (LIA-CoopNet) funded by the Centre National de Recherche Scientifique (CNRS) to G.K. This work was funded by the Institut National de la Recherche Agronomique (INRA) to HR and CD, CNRS to GK and BL, the Ministry of Agriculture to PB, Iraq government doctoral fellowship for MK and by the AgreenSkills program to SP.

List of author Contributions. HR and GK designed the research. HR supervised this project and analysed the data. GK wrote the TransDetect code. SP, MK and CD performed experiments. CD, PB and BL contributed to data analysis. BL, GK and HR wrote the manuscript.

Declaration of interest. The authors declare no competing financial interests.

Abstract

Identifying transcription factors (TFs) cooperation controlling target gene expression is still an arduous challenge. The accuracy of current methods at genome scale significantly drops with the increase in number of genes, which limits their applicability to more complex genomes, like animals and plants. Here, we developed an algorithm, TransDetect, able to predict TFs combinations controlling the expression level of a given gene. TransDetect was used to identify novel TFs modules regulating the expression of Arabidopsis phosphate transporter *PHO1;H3* comprising MYB15, MYB84, bHLH35 and ICE1. These TFs were confirmed to interact between themselves and with the *PHO1;H3* promoter. Phenotypic and genetic analyses of TF mutants enable the organization of these four TFs and *PHO1;H3* in a new gene regulatory network controlling phosphate accumulation in zinc-dependent manner. This demonstrates the reliability of TransDetect to extract directionality in non-dynamic transcriptomes and to provide blueprint to identify gene regulatory network involved in a given biological process.

Key words: Computational biology, transcription factor, mineral nutrition, phosphate, zinc

Short title: TransDetect reveals key transcription factors involved in Pi homeostasis

Summary: TransDetect uses non-dynamic transcriptomes to defining regulatory pathways controlling phosphate accumulation in zinc-deficient plants.

Introduction

Transcription factors are recognized as important orchestrators of living organisms response to environmental stimuli. Emerging experimental data indicates that a given gene in the eukaryotic genome is controlled by a high number of TFs (*e.g.* Xu et al., 2013; Kaufmann et al., 2010a). In plants, techniques including Chromatin Immuno-Precipitation (ChIP, Kaufmann et al, 2010b; Nagel et al., 2015), DAP-seq (O'Malley et al., 2016), TARGET (Medici et al., 2015; Para et al., 2014; Bargmann et al., 2013; Doidy et al, 2016), or Y1H (Brady et al., 2011; Gaudinier et al., 2011; Taylor-Teeples et al., 2015) are consistent with this potential high number of regulators, define some of the inner features of Gene Regulatory Networks (GRNs) topology. Knowing for instance that an eukaryotic genome posses ~2500 TFs, this presupposes that ~250,000 regulatory connections are pointing towards 30,000 genes. Thus, in average, a gene is likely to be under the direct influence of ~6 to 40 TFs. Hence complex interactions between TFs could determine the amplitude of the responses to different stress conditions. Despite its primary importance, so far our capacity to predict how specific TFs interact and form functional networks to regulate gene expression level is limited. Very few computational tools are able to predict TFs combinatorial effects so far. It is worth noting that while the current computational techniques are mainly based on the detection of co-occurrence of cis-regulatory elements in promoters as well as study of protein-protein interaction or Chip-Seq data none of these techniques use gene expression *per se* to extract such potential cooperation (GuhaThakurta and Stormo, 2001, Nagamine et al., 2005, Chang et al., 2006, Yu et al., 2006, Datta and Zhao, 2008, Qin et al., 2014).

In the last few years, attention has been stepped up to develop and use computational tools to decode complex TFs regulatory network involved in the regulation of complex biological process such as the coordination of nutrient signalling pathways (Rouached and Rhee, 2017). For instance, an intriguing coordination between the homeostasis of an macronutrient (phosphate, Pi) and micronutrient (zinc, Zn) respectively has been recognized in plants: Pi accumulation in the shoots is increased by Zn deficiency (-Zn) (for review, Bouain et al., 2014; Kisko et al., 2015). Nevertheless, despite its fundamental importance

the molecular basis of the over-accumulation of Pi in -Zn conditions remains elusive. In Arabidopsis, the Pi transporter *PHO1;H3* was identified as an important player in the coordination of Pi and Zn homeostasis (Khan et al., 2014). *PHO1;H3* transcript abundance specifically increases in roots upon –Zn treatment (Khan et al., 2014). Plants that do not express PHO1;H3 accumulate more Pi in the shoots than wild-type plants. PHO1;H3 is proposed to be a negative regulator of Pi translocation to the shoot in response to –Zn (Khan et al., 2014). With these characteristics, *PHO1;H3* constitutes an entry point to extend our knowledge on the molecular network regulating Pi–Zn signalling crosstalk in plants.

In this study, we developed a computational tool, named TransDetect, able to predict TFs combination controlling a given gene. We used it to identify TFs involved in the regulation of the expression of *PHO1;H3*. A reverse genetic approach was then used to functionally validate the role of the identified TFs in regulating: (i) *PHO1;H3* expression (ii) Pi accumulation in shoots in presence or absence of Zn. The interaction between the TF themselves and with *PHO1;H3* promoter was assessed using yeast two- and one-hybrid assays, respectively. Overall, this work leads us to validate the TransDetect method, and to provide a backbone for the establishment of a new regulatory network for Pi accumulation under -Zn conditions in plants. The uncovered molecular network defines an independent path from the well-established Pi-starvation signalling pathway (Bari et al., 2006; Lin et al., 2008).

Results

TransDetect: a new algorithm identifying potential regulating pair of TFs

In this study, we first undertook a computational approach designed to extract, from transcriptomic data, potential information concerning TF interaction in the control of a particular gene. The scheme of the algorithm, written in R (https://www.r-project.org/), is depicted in Figure 1. The whole process starts with the selection by the user of a particular gene (here *PHO1:H3*). Then, the script selects all the TFs having a putative binding site in the target promoter as described in Katari et al., (2010). This step can be easily bypassed in order to infer interactions of TFs that may not interact directly with the target gene or interact

with a non-canonical DNA sequence. Following this, the algorithm enters into an iterative process (Figure 1). Each pair of TFs expression in a first transcriptomic dataset (named data1) is used to fit the target expression following the equation: $Target_{data1} = \alpha TF1_{data1} + \beta TF2_{data1} + \gamma TF1_{data1} * TF2_{data1} + \varepsilon$. In this equation, $Target_{data1,}$ $TF1_{data1,}$ $TF2_{data1}$ represents the Target, TF1 and TF2 expression in the first dataset respectively $TF1_{data1} * TF2_{data1}$ represents the potential combinatorial interaction of TF1 and TF2 expressions; α, β, γ represents the coefficients of the linear modeling and ε the non-explained variance. Each model is then evaluated based on two criteria. The first one is that both TF1 and TF2 have to explain the target expression additionally or in combination. This is performed by filtering on p-values < 0.001 on [the α and the β coefficients] OR the γ alone. Any model recording the effect of only one TF is discarded since the rationale is that it can be retrieved by simple correlation network studies. The second criterion is the capacity of the fitted model to predict the target expression in a second external dataset (named data2, see Figure 1) that was not used to fit the model.

We thus use the fitted model coefficients to predict (without fitting) the Target expression, in the new conditions (data2), following the equation $Target_{data2} = \alpha TF1_{data2} + \beta TF2_{data2} + \gamma TF1_{data2} * TF2_{data2} + \varepsilon$. It then evaluates the quality of the prediction by generating the R^2 value for a linear regression between observed and predicted values (on the second dataset).

This process is iterated for all the potential TF pairs. This is necessary to find out the "best" pairs of TFs that: (i) fit the training dataset and (ii) predict gene expression in the external dataset. These models are selected if they maximize the sum of the R^2 values (default threshold 15 for the sum of the R^2 0.75 for simple R^2) in the fitted and in the predicted dataset. Thus it is possible to detect potential coordination of a gene expression by pairs of TFs. Finally each model (pair of TF) is saved. The TFs are finally ranked based of the number of times they have been found to participate in a model having passed the different criteria.

MYB15, MYB84 and bHLH35 regulate *PHO1;H3* expression under zinc deficiency

TransDetect was used to identify TFs regulating the expression of the Pi transporter *PHO1;H3* in Arabidopsis roots. The root transcriptomic dataset used for the learning step (52 data points/Affy Chips) and the root transcriptomic dataset used for the validation (69 data points/Affy Chips) are publicaly available (Brady et al, 2007; Dinneny et al, 2008; Azevedo et al, 2016). Our analysis identified a total of 165 TFs organized in pairs (Table S1) as potential regulators of *PHO1;H3*. The potential TFs network constructed based on TransDetect analysis (Figure 2) illustrates the candidate TFs pairs to regulate *PHO1;H3*, and show number of TFs are involved in more than one connection. In this study, the candidate TFs were ranked based on the number of appearances in significant models. The top ten TFs were considered for further analyses (Figure 3A)

PHO1;H3 transcript abundance is known to increase in response to –Zn condition (Khan et al, 2014). We therefore hypothesized that mutations of these TFs would affect the expression of *PHO1;H3* in response to –Zn. For each of the ten selected TFs *PHO1;H3* transcript accumulation was assessed by quantitative RT-PCR in roots of WT Col-0 plants and of two different T-DNA insertion mutant lines grown in the presence or absence of Zn for 18 days. As expected (Khan et al, 2014), -Zn treatment caused a two-fold increase of *PHO1;H3* transcripts in WT Col-0 plants (Figure 3A). Interestingly, among the twenty considered mutant lines the loss of function of members of the MYB15/MYB84 and MYB15/bHLH35 TFs pairs affect the *PHO1;H3* expression in –Zn conditions. Mutation of the two R2R3-MYB TFs *MYB15* (At3g23250) or *MYB84* (At3g49690) lead to an increase in *PHO1;H3* transcript accumulation in -Zn (Figure 3 A). This result suggests that these two TFs are negatively regulating *PHO1;H3* expression in response to a –Zn. In contrast, mutations in *bHLH35* (At5g57150) lead to a decrease in *PHO1;H3* transcript accumulation (Figure 3A), revealing a positive regulatory role of *bHLH35* (activator) on *PHO1;H3* expression in –Zn condition. *PHO1;H3* transcript accumulation was not significantly altered in plants harbouring a mutation in any of the other 7 TFs (Figure 3A). It is noteworthy that among these three TFs only *MYB15* was significantly induced in WT plants grown for 18 days in -Zn (Figure 3B).

We then tested whether *MYB15, MYB84* and *bHLH35* could interact with the promoter of *PHO1;H3*

(*pPHO1;H3*), using a yeast one-hybrid assay. Interestingly, MYB15 and MYB84 interacted with *pPHO1;H3* fragments, but bHLH35 did not (Figure 3C). It thus cannot be excluded that MYB15 and MYB84 regulate *PHO1;H3* expression independently from each other. However, bHLH35 may interact with *pPHO1;H3* through a partnership with another protein. Indeed, it cannot be ruled out that bHLH35 controls *pPHO1;H3* activity through the activation of an intermediate TF that was not identified using TransDetect.

MYB15, MYB84 and bHLH35 influence Pi accumulation in the shoot under zinc deficiency

PHO1;H3 is known to regulate the accumulation of Pi in the shoot of Zn deficient plants (Khan et al, 2014). When grown in Zn-free medium, *pho1;h3* mutant plants display a higher shoot Pi accumulation than wild-type plants, indicating that PHO1;H3 reduces Pi translocation to the shoot in response to –Zn (Khan et al, 2014). To check whether changes in *PHO1;H3* transcript accumulation in *myb15*, *myb84*, and *bhlh45* mutant backgrounds would result in changes in Pi accumulation under Zn deficiency, we determined the Pi concentration in shoots of WT (Col-0), *myb15*, *myb84*, and *bhlh35* mutant lines grown in either +Zn or -Zn conditions for 18 days As expected, Pi concentration was increased in the shoots of WT plants grown under -Zn (Figure 3D). Then, while mutations in *myb15* and *myb84* resulted in reduced Pi accumulation in shoots, mutations in *bhlh35* caused an increase in Pi accumulation (Figure 3D). These variations in shoot Pi concentration were consistent with the variations of *PHO1;H3* transcript abundance. Our results thus demonstrate the involvement of MYB15, MYB84 and bHLH35 in the regulation of Pi accumulation in the shoot of plants grown in –Zn conditions.

MYB15/MYB84 and MYB15/bHLH35 interactions are involved in the plant response to -Zn

Since the MYB15/MYB84 and MYB15/bHLH35 TFs pairs were predicted by TransDetect to cooperatively regulate *PHO1;H3* expression (Figure 4A-B), we tested whether the TFs constituting these pairs interact physically. Using a yeast two-hybrid assay, we found that MYB15 has the ability to

physically interact with MYB84 and with bHLH35 (Figure 4C). We then generated *myb15/myb84* and *myb15/bhlh35* double KO mutants in Arabidopsis by crossing single mutant lines. Interestingly, when grown in -Zn, the myb15/myb84 double mutant showed an increase of the *PHO1;H3* expression level and a decrease of Pi accumulation in the shoots compared to *myb15*, *myb84* or WT plants (Figure 4D-E). As already mentioned MYB15 and bHLH35 have opposite effects on both *PHO1;H3* expression and Pi accumulation. When grown in -Zn, the myb15/bhlh35 double mutant showed an accumulation of *PHO1;H3* transcript (Figure 4D) and Pi concentration in shoots similar to what was observed in the myb15 single mutant (Figure 4E). These results are indicative that the three TFs likely belong to the same molecular pathway regulating *PHO1;H3* in response to –Zn. It is likely that in this pathway MYB15 acts downstream bHLH35 (Figure 4D-E).

ICE1 regulates Pi accumulation under Zn deficiency in a MYB15 dependent manner.

The role of MYB15 in regulating Pi accumulation is new. However, MYB15 has been shown to physically interact with the MYC-like bHLH TF ICE1 (INDUCER OF CBP EXPRESSION 1) to regulate the plant response to cold stress (Miura et al, 2007; Agarwal et al, 2006). Through this interaction, ICE1 suppresses the activity of MYB15 (Miura et al, 2007). It is noteworthy that lowering the stringency of our TransDetect analysis revealed a potential effect of MYB15 and ICE1 as TFs pair on the expression of *PHO1;H3* (Figure 5A). We thus tested whether ICE1, individually or cooperatively with MYB15, could be involved in the regulation of *PHO1;H3* expression. First *ICE1* transcript level was found to be significantly ~2 fold induced under -Zn (Figure 5B). Then a KO mutation of *ice1* lead to a decrease in *PHO1;H3* transcript accumulation (Figure 5C) and coupled with an increase in shoot Pi concentration under -Zn when compared to WT plants (Figure 5D). The *myb15/ice1* double mutant displayed increased *PHO1;H3* transcript accumulation (Figure 5C) and a decreased Pi concentration in shoots in response to -Zn, in a similar range as what was observed in the single *myb15* mutant (Figure 5D). Our results thus indicate that MYB15 most probably acts downstream ICE1 to control Pi accumulation under -Zn *via*

190 *PHO1;H3*.

191 **Discussion.**
192
193 Gene expression data is increasing with the use of transcriptomic technologies, requiring the development
194 of methods for their efficient analysis. Combination with functional genomics approaches these
195 computational tools can help to gain new insight on the molecular mechanisms of complex phenomenon
196 such as the regulation of ions homeostasis in plants (Mongon et al, 2017; Rouached and Rhee, 2017). In
197 this context, we developed and used an algorithm, TransDetect, to identify regulators (TFs) and to build
198 a GRNs that control the expression of a Pi transporter, *PHO1;H3*, in response to -Zn conditions.
199 In Arabidopsis, the *PHO1;H3* gene was demonstrated to be involved in the coordination of Pi and Zn
200 homeostasis (Khan et al, 2014). The expression of *PHO1;3* is induced in response to -Zn treatments in
201 roots (Khan et al, 2014). Mutation of *PHO1;H3* causes an overaccumulation of Pi in Arabidopsis shoots
202 (Khan et al, 2014). Therefore, *PHO1;H3* gene was proposed to plays a negative regulatory role of Pi
203 transfer from root to shoots in -Zn conditions (Khan et al, 2014). Nevertheless, the GRN that regulates
204 the expression of *PHO1;H3* in response to -Zn still unknown. Using TransDetect algorithm, we identified
205 a list of candidate TFs pair for the regulation of the *PHO1;H3* expression. Among the top 10 candidates
206 revealed by TransDetect, we tested 20 mutant lines (2 mutant per TFs) among which 3 display interesting
207 phenotypes related to *PHO1;H3* expression (Figure 3 A-B). We believe that this relatively high level of
208 success could be explained as follow: in general, algorithms focusing on correlation between genes do
209 not provide any information concerning causality. Say that if 2 genes A and B are highly correlated, it
210 does not imply if A→B or if B→A. Dynamic aspects can sort between the 2 situations (Krouk et al, 2013).
211 Unfortunately, the vast majority of the transcriptome in databases are not kinetics. We would like to
212 mention here that, by the way TransDetect is working, it might extract some directionally information
213 from static data. To clearly explain this, consider the ideal case where 2 TFs (TFA and TFB) control a
214 Target gene following a logic gate (Figure 6). In this particular case, γ coefficient of the linear model will
215 be highly significant because it is the combination of TFA and TFB expression that is necessary to fully

explain Target transcript level. On the other hand, it is not possible to infer TFA by a linear combination of Target and TFB, nor to explain TFB by a linear combination of Target and TFA. Thus, the term of the equation γTFA*TFB intrinsically possess some directionality explanatory power. It is important to note that this directionality will occur only when some interactions between the explanatory variables exist. Since the TransDeTect algorithm favours models having a significant interaction term between TFs, we believe that this particularity might explain its availability to infer actual regulators. Thus, we propose that TransDetect is suitable to discover TFs that coordinate the expression of any gene or set of genes of interest. It worth noting that although microarray data were used in this study, TransDetect algorithm could also use value of mRNA level obtained from RNA-seq experiments. While ICE1 and MYB15 was not detected as TFs pair using our set-up of fitting and predicting dataset, it was detected by lowering the threshold. Therefore, testing different fitting and predicting dataset set-up on one hand, and changing threshold on another had, could help reaching conclusion on possible detection TFs pairs. In the frame of this study, beside *PHO1;H3*, the use of TransDetect and based on TF ranking (counting the number of times that a particular TF appears in a model), which is a crucial step in the algorithm, known TFs and their targets could be retrieved. For instance, TransDetect retrieved TF and target gene involved in the regulation of root development (e.g. DNA BINDING WITH ONE FINGER 53 (DOF53, At5g60200) its targets *REVOLUTA* (*REV*, At5g60690)) (Brady et al, 2011), secondary cell wall synthesis (e.g. ARABIDOPSIS THALIANA HOMOLOG OF E2F C TF (E2Fc, At1g47870) and its target *ASCULAR RELATED NAC-DOMAIN PROTEIN 7* (*VND7*, At1g71930) (Taylor-Teeples et al, 2015), and iron transport (POPEYE (PYE, At3g47640) and its target *IRON-REGULATED TRANSPORTER 1* (*IRT1*, At4g19690)) (Long et al, 2010) (Supplementary Figure 1). These data further support the utility of TransDetect to detect TFs. The validation of detected TFs require *in planta* and biochemical testing, which would include the analysis of expression profiles of the target genes in different plant genetic backgrounds (eg wild-type plants, knock-out mutants /or overexpressing lines). As performed in this work, transcriptionally linked TFs and promoter of target genes could be further tested for their possible direct

241 interaction.

242

243 Current understanding of adaptive mechanisms regulating Pi homeostasis in plants comes from
244 investigations conducted mainly in *Arabidopsis thaliana* under Pi limitation. From twenty years of
245 research only a handful of TFs (for review Jain et al, 2012) and only one complete Pi signalling pathway,
246 the "PHR1- miR399-PHO2" pathway (Bari et al, 2006; Lin et al, 2008) have been discovered.
247 Nevertheless, as aforementioned, Pi accumulation in shoot is altered when plants are challenged by Zn
248 limitation, and this alteration is not dependent from the "PHR1-miR399-PHO2" regulatory pathway
249 (Khan et al, 2014). These observations indicate the existence of specific regulatory pathway(s) underlying
250 this Zn-Pi relationship (Khan et al, 2014). Unfortunately, available tools do not offer the possibility to
251 identify the TF pairs involved in such nutrient homeostasis coordination. Thanks to TransDetect used to
252 search for TFs controlling Pi homeostasis through the examination of the publically available
253 transcriptomic data sets with *PHO1;H3* as target gene we identified four new TF (MYB15, MYB84,
254 bHLH35 ICE1) displaying a striking phenotype with regards to both *PHO1;H3* expression and shoot Pi
255 accumulation in plant grown under –Zn. Considering that only a handful of TFs involved in the
256 transcriptional control of plant response to Pi or Zn deficiency were described before this study (Assunção
257 et al, 2010; Jain et al, 2012; Khan et al, 2014), one can consider that in this regard the success rate of this
258 strategy - combining TransDetect together with functional genomics approaches - is high. More
259 importantly, integration of these data provide blueprint for defining novel regulatory pathway controlling
260 Pi homeostasis in plants. Using the phenotypic data obtained from the characterisation of single and
261 double mutant TF mutants effect on the expression of *PHO1;H3* it was possible to propose a new
262 regulatory transcriptional module regulating Pi accumulation in shoot of Zn-deficient plants (Figure 7).
263 In this module, MYB15, MYB84 are likely to play a negative regulatory role on the expression of
264 *PHO1;H3*, while ICE1 bHLH35 plays a positive regulatory role upstream MYB15 (Figure 7). This work
265 thus lead to the identification of new key players that act in the -Zn signalling pathways to control the

expression of *PHO1;H3* and Pi accumulation in plants, which is indeed independent of the PHR1-miR399-PHO2 pathway constituents.

In conclusion, this work identified four new TFs acting to regulate Pi accumulation in Arabidopsis in response to Zn deficiency. Prediction using TransDetect was validated using three different strategies First, molecular and genetic evidences showing the involvement of the selected TFs in modulating *PHO1;H3* expression in response to –Zn. Second, yeast-one and two-hybrid experiments shows that these TFs can interact with the *PHO1;H3* promoter, that they are able to form TF pairs. Finally, these TF pairs are involved in the regulation of Pi accumulation in plants under –Zn conditions. The method developed in the frame of this work should benefit to other studies aiming at identifying TFs cooperatively regulating a gene(s) expression, and to dissect regulatory pathway(s) controlling an important biological phenomenon.

Materials Methods

Algorithm

The TransDetect algorithm as been written in R (https://wwwr-projectorg/) and it follows the exact logic described in Figure 1. The R code is available at https://sites.google.com/site/gabrielkroukresearch/transdetect. The running time is about 20 minutes per target gene on a desktop Apple Mac Pro computer with parallelized computation on 32 CPUs. The transcriptomic dataset used is from the Benfey lab (Brady et al, 2007; Dinneny et al, 2008; Azevedo et al, 2016) and has been spited arbitrarily into fitting (52 chips) and predicting dataset (69 chips).

Plant materials and growth conditions

The *Arabidopsis thaliana* mutants used in all experiments were in the Columbia (Col-0) genetic background. The previously described *ice1-2* (At3g26744) mutant (Denay et al, 2014) was provided by Dr Gwyneth Ingram (ENS, Lyon, France). T-DNA insertion mutant lines for considered TFs At5g57150 (line1: N516841 and line2: N536664); At3g23250 (line1: N651976 and line2: N491226); At3g49690

(line1: N641918 and line2: N612398); At4g37790 (N585964, N2100629); At2g46510 (N587068, N867699); At1g31050 (N595172; N545538); At5g04760 (N2101152, N2104259); At4g31800 (N550079, N871514); At4g24060 (N652104, N504243) and At3g50060 (N567655, N555373) were from Nottingham Arabidopsis Stock Centre (Alonso et al, 2003). The presence of a T-DNA insertion within the TF gene and absence of transcripts of the mutated TFs were checked using the appropriate PCR strategy using PCR primers listed in Table S2. Double mutant lines *myb15/myb84*, *myb15/bhlh35*, and *ice1/myb15* were generated through crossing. Homozygosity of the generated double mutants was confirmed through appropriate PCR strategy as performed for the identification of the single mutants. Plants were germinated grown in vertical position on 1% agar-solidified media (A1296, Sigma) The complete nutrient medium contained 05 mM KNO_3, 1 mM $MgSO_4$, 1 mM KH_2PO_4, 025 mM $Ca(NO_3)_2$, l00 µM NaFeEDTA, 30 µM H_3BO_3, l0 µM $MnCl_2$, l µM $CuCl_2$, 15 µM $ZnSO_4$, 01 µM $(NH_4)6Mo_7O_{24}$, 50 µM KCl, pH 5.7. Zn-free medium was made by removing the only source of Zn ($ZnSO_4$), by washing the agar Seeds were sown on the plates stratified at 4 °C in the dark for 3 d. Plates were then transferred in a growth chamber for 18 d, day 1 of growth being defined as the first day of exposure of stratified seeds to light. Plants were grown under long-day conditions (16/8h light/dark cycle, 250 µmol·m^{-2}·s^{-1}, 24/20°C).

Phosphate quantification

Shoots and roots were collected separately. Shoots were weighed and ground into powder in liquid nitrogen, then incubated at 70 °C for ½ hour. The determination of Pi concentrations in these tissues was performed using the Ames methods (1996). For every measurement, three to five biological replicates (3 plants per sample) were performed, leading to three to five corresponding samples.

Real-time quantitative reverse-transcription PCR

Roots of 18-day-old plants grown on different medium composition in the presence or absence of Zn were collected for gene expression analysis. Total RNA was extracted from 100 mg frozen roots using Plant

RNeasy extraction kit (Qiagen) and RQ1 RNAse-free DNAse (Promega). Two µg of total RNA were used to synthesize cDNA using poly-A oligos. Real-time quantitative reverse-transcription PCR (RT-qPCR) was performed with a Light Cycler 480 Real-Time PCR System using SYBR green dye technology (Roche) as described previously (Rouached et al, 2011). The *PHO1;H3* transcript abundance were quantified using quantitative real time PCR using specific primers listed in Table S2, which showed an efficiency (E) of 100% ± 3%. *E* was determined after the analysis of serial 1:10 dilutions of a plasmidic solution of each target gene by using the equation $E = [(10^{-1/s}) - 1] \cdot 100$. In this equation "s" represent the slope of the linear regression of the threshold cycle (C_T) values per the $\log_{10}$ values of DNA copy numbers used for PCR reactions (Rouached et al, 2008). Relative transcripts levels was quantified using the comparative threshold cycle (C_T) method (Livak Schmittgen, 2001). For every data point, C_T value was the average of the C_T values obtained from the triplicate PCR analysis. For each gene, the relative amount of calculated mRNA was normalized to the level of the control gene *Ubiquitin10* (*UBQ10*: At4g05320) and expressed as relative values against wild-type plants grown in reference treatment (RT: +Zn) medium. For example, relative gene expression of the *PHO1;H3* genes $\Delta C_{T,PHO1;H3}$ was expressed following normalization against the average of the C_T values obtained for the gene used for stardization: $\Delta C_{T,PHO1;H3} = C_{T,PHO1;H3} - C_{T,UBQ10}$ (Livak Schmittgen, 2001). For treatment of interest (TOI: -Zn) was compared to a reference treatment (RT: +Zn), the relative expression of a *PHO1;H3* gene was expressed as a ΔΔCt value calculated as follows: $\Delta\Delta Ct = \Delta C_{T,TOI} - \Delta C_{T,RT}$ (Livak Schmittgen, 2001). The fold change in relative gene expression was determined as $2^{-\Delta\Delta CT}$. Using this method, +Zn values were normalized to 1. The methodology apply for the analysis of relative expression of the other genes: *MYB15*, *ICE1*, *BHLH35* and *MYB84*.

Yeast experiments

All the PCR products were obtained using high-fidelity Phusion DNA polymerase. The constructs were sequenced to ensure their integrity. All primers used for yeast one-hybrid (Y1H) and two-hybrid (Y2H)

experiments are described in table S2. For Y1H experiments bHLH35 (At5g57150) cDNA was PCR-amplified from a pool of Columbia (Col-0) cDNA using the cbHLH35-B1 and cbHLH35-B2 primers, introduced into the pDONR207 vector (BP recombination, Gateway®), and then recombined into the pDEST22 vector (LR recombination, Gateway®) allowing the expression of bHLH35 fused to the GAL4 activation domain (AD) in yeast pDEST22. Clones containing MYB15 (At3g23250) and MYB84 (At3g49690) were obtained from a previous study (Kelemen et al, 2015). In order to assess if bHLH35, MYB15 and MYB84 could interact with the different MYB (seven) and bHLH (one) putative binding site present on the *PHO1;3* promoter, each one was separately cloned as hexamers into the pHis-LIC vector (Kelemen et al, 2015). Subsequent interaction assays were carried out as described in (Dubos et al, 2014). For Y2H experiments, bHLH35, MYB15 MYB84 were LR recombined into pDEST32 allowing fusion with the GAL4 DNA binding domain (BD). Each pDEST22 and pDEST32 vector containing either bHLH35, MYB15 or MYB84 were transformed alone or in two-by-two combination into yeast (AH109 strain, Clontech). Subsequent steps were carried out accordingly to manufacturer's instructions using the ADE2 HIS3 reporter genes (Clontech).

Statistical analysis

Statistical differences between genotypes were calculated using t-test analyses and ANOVA with subsequent post hoc tests using Graphpad Prism (GraphPad Software Inc, San Diego, CA, USA) or Microsoft Excel (Microsoft, USA).

Supplemental Data

Table S1 AGI number occurrence in TransDetect analysis for *PHO1;H3* (At1g14040).

Table S2 List of primers used in this work.

Supplemental Figure 1. TransDetect prediction of regulators for *REVOLUTA*, *ASCULAR RELATED NAC-DOMAIN PROTEIN 7 and IRON-REGULATED TRANSPORTER 1*.

Acknowledgments. The authors are thankful to Dr Gwyneth Ingram (ENS, Lyon, France) for providing seeds of *ice1* mutant. The authors are thankful to Dr Pascal Schläpfer (Carnegie Institution for Science, Stanford, CA, USA) for very helpful discussions.

372 **Figures Legends**

373 **Figure 1. Scheme of TransDetect algorithm organization.** The algorithm is built on a inference
374 iterative process. First the target gene transcript level is fitted by a linear combination of the transcript
375 levels of two transcription factors (TFs). The resulting model is kept only if the two TFs significantly
376 participate in the fit. The learnt coefficients are then used to predict the transcript levels of the target gene
377 in an independent dataset. If the model is able to properly fit the transcript levels of the target gene in the
378 first dataset and predict them in the second dataset, the corresponding TF pair is kept. A final list of
379 selected TF pairs is generated and TFs are ranked based on the number of times they appear in this list.

380
381 **Figure 2. TransDetect network potentially influencing *PHO1;H3* gene expression.** Each node
382 represent a potential *PHO1;H3* regulator based on the TransDetect criteria defined in the text. If a pair of
383 TF is predicted to explain *PHO1;H3* expression it is linked by an edge. The edge width is proportional to
384 the sum of the R^2 for the fit and predict processes (values are ranging from 16 to 176). The most influential
385 factors are likely to be the most connected.

386
387 **Figure 3. MYB15, MYB84 and bHLH35 regulate both the expression of *PHO1;H3* and the**
388 **accumulation of Pi in the shoot under zinc deficiency. A**- Relative *PHO1;H3* (At1g14040) transcript
389 accumulation in the roots of wild-type plants (Col-0) and mutant lines harbouring loss-of-function
390 mutations in the following transcription factors: At5g57150 (*bHLH35*), At3g23250 (*MYB15*), At3g49690
391 (*MYB84*), At4g37790 (*HAT22*), At2g46510 (*bHLH17*), At1g31050 (*bHLH111*), At5g04760 (*MYB-type*),
392 At4g31800 (*WRKY18*), At4g24060 (*Dof46*) and At3g50060 (*MYB77*). Plants were grown for 18 days in
393 the presence (+Zn) or absence (-Zn) of zinc. *PHO1;H3* transcript abundance was measured by qRT-PCR
394 normalized against *UBQ10* (At4g05320). **B**- *MYB15, MYB84* and *bHLH35* transcripts accumulation in
395 response to Zn deficiency. Relative *MYB15, MYB84* and bHLH35 transcript accumulation was quantified
396 in roots of wild-type plants (Col-0) grown for 18 days in the presence or absence of Zn by qRT-PCR and
397 normalized against *UBQ10*. **C**- Yeast one-hybrid assay. Sequences of the Arabidopsis *PHO1;H3*

promoter fused to the *HIS3* auxotrophic marker were stably transformed into yeast. These different yeast strains were then co-transfected with MYB15, MYB84 or bHLH35. Left panel, growth of the different yeast strains on control media deprived of tryptophan (-W), allowing the selection of yeast cells expressing the selected TFs. Right panel, growth of the different yeast strains on selective media deprived of tryptophan and histidine (-W -H). **D**- Pi concentrations measured in the shoots of wild type, *myb15*, *myb84*, or *bhlh35* plants grown for 18 days in the presence or absence of Zn. For A, C and D panels, central lines in the boxes show the medians; box limits indicate the 25th and 75th percentiles; whiskers extend 15 times the interquartile range from the 25th and 75th percentiles Letters a, b and c indicate significantly different values at p <005 determined by one-way ANOVA and Tukey HSD.

Figure 4. Interactions between MYB15 and MYB84 and between MYB15 and bHLH35 influence the expression of *PHO1;H3* Pi accumulation under zinc deficiency. A, **B**- TransDetect prediction of correlation between the expression of the *MYB15* / *MYB84* and *MYB15* / *bHLH35* TF pairs and the *PHO1;H3* transcript level with R^2=075 and R^2=084 respectively. **C**- Yeast two-hybrid assay bHLH35, MYB15 and MYB84 were fused with either the GAL4 DNA binding domain (BD) or the GAL4 activation domain (AD) into appropriate expression vectors, which were then transferred into yeast. The different yeast strains were plated on non-selective medium (NS) or on selective media deprived of histidine (-His), adenine (-Ade) or both simultaneously (-His-Ade). **D**- Relative *PHO1;H3* transcript accumulation in roots of wild type (Col-0), *bhlh35*, *myb15*, *myb84*, *myb15*/*myb84* *myb15*/*bhlh35* mutant plants grown for 18 days in the absence of zinc (-Zn) compared to +Zn. *PHO1;H3* transcript abundance was measured by qRT-PCR and normalized against *UBQ10.* **E**- Shoot Pi concentrations measured in wild-type (Col-0), *bhlh35*, *myb15*, *myb84*, *myb15*x*myb84* and *myb15*x*bhlh35* mutant plants grown on either +Zn or –Zn for 18 days. For D and E panels, Box central lines show the medians; box limits indicate the 25th and 75th percentiles; whiskers extend 15 times the interquartile range from the 25th and 75th percentiles Letters a, b and c indicate significantly different values at p <005 determined by one-way ANOVA and Tukey HSD.

Figure 5. The ICE1 / MYB15 transcription factor pair regulates both the expression of *PHO1;H3* the accumulation Pi under –Zn. A- TransDetect's prediction of the correlation between the expression of the TF pair MYB15 and ICE1 and the *PHO1;H3* expression (R^2=0,73). **B**- *ICE1* transcript accumulation. Expression of *ICE1* was quantified in wild-type (Col-0) seedlings grown for 18 days in presence (+Zn) or absence (-Zn) of zinc. *ICE1* transcript abundance was measured by qRT-PCR normalized against *UBQ10*. **C**- *PHO1;H3* transcript accumulation. Expression of *PHO1;H3* gene was quantified in wild type (Col-0), *ice1, myb15* and *myb15/ ice1* seedlings grown for 18 days in +Zn or –Zn. *PHO1;H3* transcript abundance was measured by qRT-PCR and normalized against *UBQ10*. **D**- Pi accumulations. Pi concentrations were measured from shoots of wild type (Col-0), *ice1*, *myb15,* and *myb15* /*ice1* seedlings grown for 18 days in presence +Zn or –Zn. For B, C and D, Box center lines show the medians; box limits indicate the 25th and 75th percentiles; whiskers extend 15 times the interquartile range from the 25th and 75th percentiles. Letters a, b and c indicate significantly different values at p<005 determined by one-way ANOVA and Tukey HSD.

Figure 6. Idealized model to explain how TransDetect extract directionality in static data. A- Two transcription factors TFA and TFB positively control the expression of a Target gene TA following a AND logic-gate. **B**- TA expression is induced only when TFA and TFB expression are both upregulated. **C**- Linear modelling of TA expression. Considering the ideal case where 2 transcription factors (TFA and TFB) control a target gene TA following a AND logic-gate. In this particular case, γ coefficient of the linear model will be highly significant because it is the combination of TFA and TFB expression that is necessary to fully explain TA expression. On the other hand, it is not possible to infer TFA by a linear combination of TA and TFB, nor to explain TFB by a linear combination of TA and TFA. Thus the term of the equation γTFA*TFB intrinsically possess some directionality explanatory power in this case where both TFs interact in the control of TA.

Figure 7. Schematic representation of the MYB15, MYB84, bHLH35 and ICE1 regulatory module controlling *PHO1;H3* gene expression and Pi accumulation in shoots under zinc deficiency. Phosphate increases in the shoots of plants exposed to zinc deficiency. *PHO1;H3* plays a negative regulatory role in this process. Red solid lines indicate connections between MYB15, MYB84, bHLH35 and ICE1. Negative and positive regulatory effects of these transcription factors on *PHO1;H3* expression under zinc deficiency are indicated by flat-ended dashed lines and arrowheads, respectively. a indicates previous knowledge on ICEI and MYB15 physical interaction.

Supplementary Figure 1. TransDetect prediction of regulators for *REVOLUTA*, *ASCULAR RELATED NAC-DOMAIN PROTEIN 7 and IRON-REGULATED TRANSPORTER 1*. TransDetect was used to predict regulators for the following target genes A- *REVOLUTA* (*REV*, At5g60690), B- *ASCULAR RELATED NAC-DOMAIN PROTEIN 7* (*VND7*, At1g71930), and C- *IRON-REGULATED TRANSPORTER 1* (*IRT1*, At4g19690). Among number of TFs predicted, TransDetect retrieved known regulators for theses genes, namely DNA BINDING WITH ONE FINGER 53 (DOF53, At5g60200) for *REV*, ARABIDOPSIS THALIANA HOMOLOG OF E2F C TF (E2Fc, At1g47870) for *VND7*, and POPEYE (PYE, At3g47640) for *IRT1*.

References

Agarwal M, Hao Y, Kapoor A, Dong C-H, Fujii H, Zheng X, Zhu, J-K (2006) A R2R3 type MYB transcription factor is involved in the cold regulation of CBF genes in acquired freezing tolerance. J Biol Chem **281:** 37636-37645

Alonso JM, Stepanova AN, Leisse TJ, Kim CJ, Chen H, Shinn P, Stevenson DK, Zimmerman J, Barajas P, Cheuk R (2003) Genome-wide insertional mutagenesis of *Arabidopsis thaliana*. Science **301:**653-657

Ames BN (1966) Assay of inorganic phosphate, total phosphate and phosphatases. Methods Enzymol. **8:** 115-118

Assunção AG, Herrero E, Lin Y-F, Huettel B, Talukdar S, Smaczniak C, Immink RG, Van Eldik M, Fiers M, Schat H (2010) Arabidopsis thaliana transcription factors bZIP19 and bZIP23 regulate the adaptation to zinc deficiency Proc Natl Acad Sci **107:** 10296-10301

Azevedo H, Azinheiro SG, Muñoz-Mérida A, Castro PH, Huettel B, Aarts MM, Assunção AG (2016) Transcriptomic profiling of Arabidopsis gene expression in response to varying micronutrient zinc supply. Genom data **7:** 256-258

Bargmann BO, Marshall-Colon A, Efroni I, Ruffel S, Birnbaum KD, Coruzzi GM, Krouk G (2013) TARGET: a transient transformation system for genome-wide transcription factor target

481 discovery. Mol Plant **6:** 978-980
482 **Bari R, Pant BD, Stitt M, Scheible W-R** (2006) PHO2, microRNA399, PHR1 define a phosphate-
483 signaling pathway in plants. Plant Physiol: **141.** 988-999
484 **Bouain N, Shahzad Z, Rouached A, Khan GA, Berthomieu P, Abdelly C, Poirier Y, Rouached H**
485 (2014) Phosphate and zinc transport and signalling in plants: toward a better understanding of
486 their homeostasis interaction. J Exp Bot **65:** 5725-5741
487 **Brady SM, Orlo DA, Lee J-Y, Wang JY, Koch J, Dinneny JR, Mace D, Ohler U, Benfey PN** (2007)
488 A high-resolution root spatiotemporal map reveals dominant expression patterns. Science **318:**
489 801-806
490 **Brady SM, Zhang L, Megraw M, Martinez NJ, Jiang E, Charles SY, Liu W, Zeng A, Taylor-Teeples**
491 **M, Kim D** (2011) A stele-enriched gene regulatory network in the Arabidopsis root. Mol Syst
492 Biol **7:** 459
493 **Chang Y-H, Wang Y-C, Chen B-S** (2006) Identification of transcription factor cooperativity via
494 stochastic system model. Bioinformatics **22:** 2276-2282
495 **Datta D, Zhao H** (2008) Statistical methods to infer cooperative binding among transcription factors in
496 *Saccharomyces cerevisiae*. Bioinformatics **24:** 545-552
497 **Denay G, Creff A, Moussu S, Wagnon P, Thévenin J, Gérentes M-F, Chambrier P, Dubreucq B,**
498 **Ingram, G** (2014) Endosperm breakdown in Arabidopsis requires heterodimers of the basic
499 helix-loop-helix proteins ZHOUPI INDUCER OF CBP EXPRESSION 1. Development **141:**
500 1222-1227
501 **Dinneny JR, Long TA, Wang JY, Jung JW, Mace D, Pointer S, Barron C, Brady SM, Schiefelbein**
502 **J, Benfey PN** (2008) Cell identity mediates the response of Arabidopsis roots to abiotic stress.
503 Science **320:** 942-945
504 **Doidy J, Li Y, Neymotin B, Edwards MB, Varala K, Gresham D, Coruzzi GM** (2016) Hit-and-Run"
505 transcription: de novo transcription initiated by a transient bZIP1 "hit" persists after the "run".
506 BMC genomics **17:** 1
507 **Dubos C, Kelemen Z, Sebastian A, Bülow L, Huep G, Xu W, Grain D, Salsac F, Brousse C, Lepiniec,**
508 **L** (2014) Integrating bioinformatic resources to predict transcription factors interacting with cis-
509 sequences conserved in co-regulated genes. BMC genomics **15:** 1
510 **Gaudinier A, Zhang L, Reece-Hoyes JS, Taylor-Teeples M, Pu L, Liu Z, Breton G, Pruneda-Paz,**
511 **JL, Kim D, Kay SA** (2011) Enhanced Y1H assays for Arabidopsis. Nature methods **8:** 1053-
512 1055
513 **GuhaThakurta D, Stormo GD** (2001) Identifying target sites for cooperatively binding factors.
514 Bioinformatics **17:** 608-621
515 **Jain A, Nagarajan VK, Raghothama KG** (2012) Transcriptional regulation of phosphate acquisition by
516 higher plants. Cell Mol Life Sci **69:** 3207-3224
517 **Katari MS, Nowicki SD, Aceituno FF, Nero D, Kelfer J, Thompson LP, Cabello JM, Davidson RS,**
518 **Goldberg AP, Shasha DE** (2010) VirtualPlant: a software platform to support systems biology
519 research. Plant Physiol **152:** 500-515
520 **Kaufmann K, Pajoro A, Angenent GC** (2010a) Regulation of transcription in plants: mechanisms
521 controlling developmental switches. Nat Rev Genet **11:** 830-842
522 **Kaufmann K, Muino JM, Østerås M, Farinelli L, Krajewski P, Angenent GC** (2010b) Chromatin
523 immunoprecipitation (ChIP) of plant transcription factors followed by sequencing (ChIP-SEQ)
524 or hybridization to whole genome arrays (ChIP-CHIP). Nature Protocols **5:** 457-472
525 **Kelemen Z, Sebastian A, Xu W, Grain D, Salsac F, Avon A, Berger N, Tran J, Dubreucq B, Lurin**
526 **C** (2015) Analysis of the DNA-Binding Activities of the Arabidopsis R2R3-MYB Transcription
527 Factor Family by One-Hybrid Experiments in Yeast. PloS One **10:** e0141044
528 **Khan GA, Bouraine S, Wege S, Li Y, De Carbonnel M, Berthomieu P, Poirier Y, Rouached H** (2014)

Coordination between zinc and phosphate homeostasis involves the transcription factor PHR1, the phosphate exporter PHO1, its homologue PHO1; H3 in Arabidopsis. J Exp Bot **65:** 871-884

Krouk G, Lingeman J, Colon AM, Coruzzi G, Shasha D (2013) Gene regulatory networks in plants: learning causality from time perturbation. Genome biol **14:** 1

Lin S-I, Chiang S-F, Lin W-Y, Chen J-W, Tseng C-Y, Wu P-C, Chiou T-J (2008) Regulatory network of microRNA399 and PHO2 by systemic signalling. Plant Physiol **147:** 732-746

Livak KJ, Schmittgen TD (2001) Analysis of relative gene expression data using real-time quantitative PCR the 2− ΔΔCT method. Methods **25:** 402-408

Long TA, Tsukagoshi H, Busch W, Lahner B, Salt DE, Benfey PN (2010) The bHLH transcription factor POPEYE regulates response to iron deficiency in Arabidopsis roots. Plant Cell **22:** 2219-2236

Medici A, Marshall-Colon A, Ronzier E, Szponarski W, Wang R, Gojon A, Crawford NM, Ruffel S, Coruzzi GM, Krouk G (2015) AtNIGT1/HRS1 integrates nitrate and phosphate signals at the Arabidopsis root tip. Nat Commun **6:** 6274

Miura K, Jin JB, Lee J, Yoo CY, Stirm V, Miura T, Ashworth EN, Bressan RA, Yun D-J, Hasegawa PM (2007) SIZ1-mediated sumoylation of ICE1 controls CBF3/DREB1A expression freezing tolerance in Arabidopsis. Plant Cell **19:** 1403-1414

Mongon J, Chaiwong N, Bouain N, Prom-u-Thai C, Secco D, Rouached H (2017) Phosphorus and iron deficiencies influences Rice Shoot Growth in an Oxygen Dependent Manner: Insight from Upl Lowl rice. IJMS **18:** 607

Nagamine N, Kawada Y, Sakakibara Y (2005) Identifying cooperative transcriptional regulations using protein–protein interactions. Nucleic Acids Res **33:** 4828-4837

Nagel DH, Doherty CJ, Pruneda-Paz JL, Schmitz RJ, Ecker JR, Kay SA (2015) Genome-wide identification of CCA1 targets uncovers an exped clock network in Arabidopsis. Proc Natl Acad Sci **112:** E4802-E4810

O'Malley RC, Huang S-sC, Song L, Lewsey MG, Bartlett A, Nery JR, Galli M, Gallavotti A, Ecker JR (2016) Cistrome Epicistrome Features Shape the Regulatory DNA Lscape. Cell **165:** 1280-1292

Para A, Li Y, Marshall-Colón A, Varala K, Francoeur NJ, Moran TM, Edwards MB, Hackley C, Bargmann BO, Birnbaum KD (2014) Hit--run transcriptional control by bZIP1 mediates rapid nutrient signaling in Arabidopsis. Proc Natl Acad Sci **111:** 10371-10376

Qin J, Hu Y, Xu F, Yalamanchili HK, Wang J (2014) Inferring gene regulatory networks by integrating ChIP-seq/chip transcriptome data via LASSO-type regularization methods. Methods **67:** 294-303

Riechmann, JL, Heard, J, Martin, G, Reuber, L, Jiang, C, Keddie, J, Adam, L, Pineda, O, Ratcliffe OJ, Samaha RR, Creelman R, Pilgrim M, Broun P, Zhang JZ, Ghehari D, Sherman BK, Yu G (2000) Arabidopsis transcription factors: genome-wide comparative analysis among eukaryotes. Science **290:** 2105-2110

Rouached H, Rhee SY (2017) System-level understanding of plant mineral nutrition in the big data era. Curr Opin Syst Biol. **4:** 71-77

Rouached H, Stefanovic A, Secco D, Bulak Arpat A, Gout E, Bligny R, Poirier Y (2011) Uncoupling phosphate deficiency from its major effects on growth transcriptome via PHO1 expression in Arabidopsis. Plant J **65:** 557-570

Rouached H, Wirtz M, Alary R, Hell R, Arpat AB, Davidian J-C, Fourcroy P, Berthomieu P (2008) Differential regulation of the expression of two high-affinity sulfate transporters, SULTR1 ;1 and SULTR1 ;2, in Arabidopsis. Plant Physiol **147:** 897-911

Taylor-Teeples M, Lin L, de Lucas M, Turco G, Toal T, Gaudinier A, Young N, Trabucco G, Veling M, Lamothe R (2015) An Arabidopsis gene regulatory network for secondary cell wall synthesis. Nature **517:** 571-575

Xu W, Grain D, Gourrierec J, Harscoët E, Berger A, Jauvion V, Scagnelli A, Berger N, Bidzinski P, Kelemen Z (2013) Regulation of flavonoid biosynthesis involves an unexpected complex

transcriptional regulation of TT8 expression, in Arabidopsis. New Phytol **198:** 59-70

Yu X, Lin J, Zack DJ, Qian J (2006) Computational analysis of tissue-specific combinatorial gene regulation: predicting interaction between transcription factors in human tissues. Nucleic Acids Res **34:** 4925-4936

Figure 1

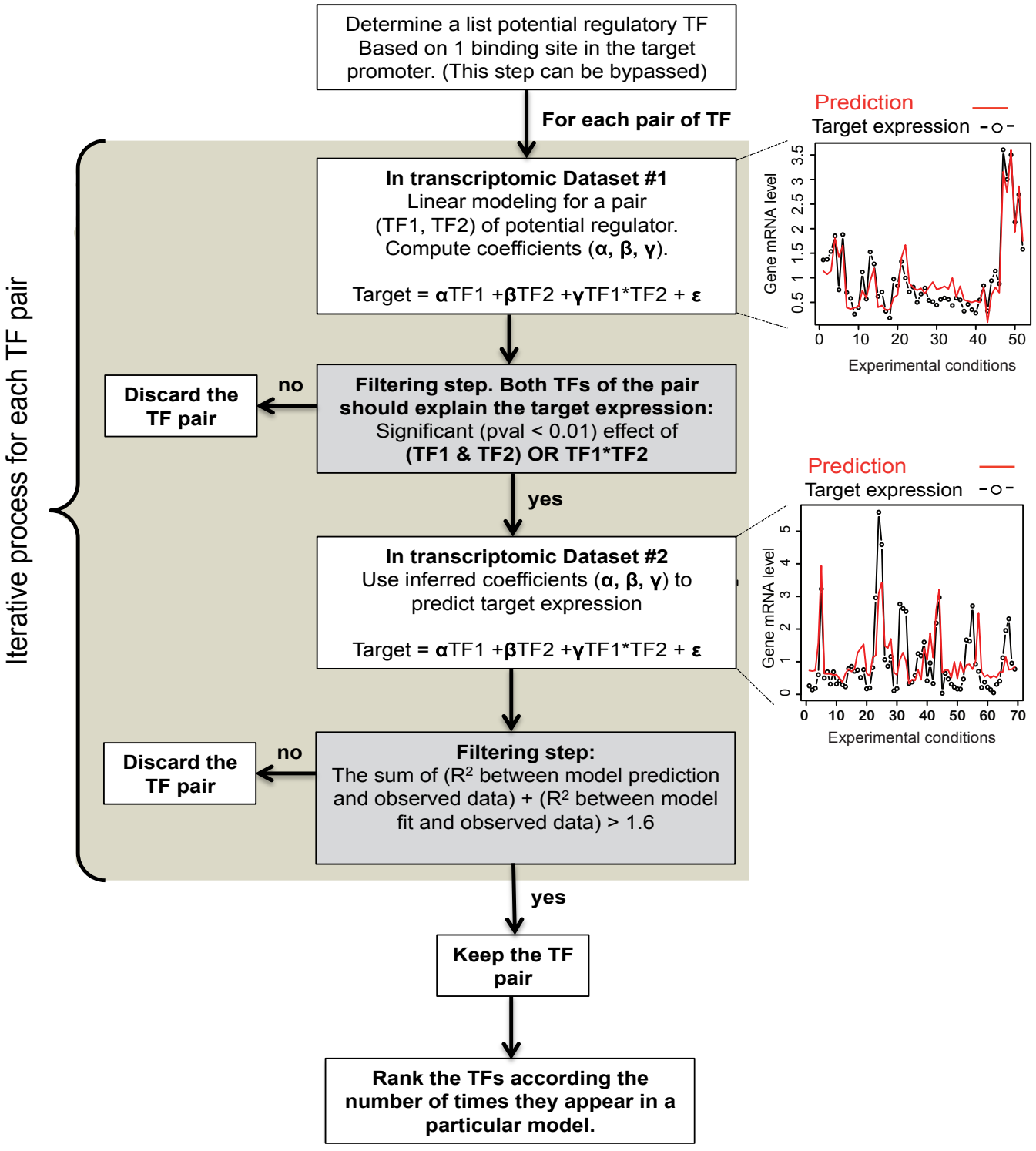

Figure 1. Scheme of TransDetect algorithm organization. The algorithm is built on a inference iterative process. First the target gene transcript level is fitted by a linear combination of the transcript levels of two transcription factors (TFs). The resulting model is kept only if the two TFs significantly participate in the fit. The learnt coefficients are then used to predict the transcript levels of the target gene in an independent dataset. If the model is able to properly fit the transcript levels of the target gene in the first dataset and predict them in the second dataset, the corresponding TF pair is kept. A final list of selected TF pairs is generated and TFs are ranked based on the number of times they appear in this list.

Figure 2

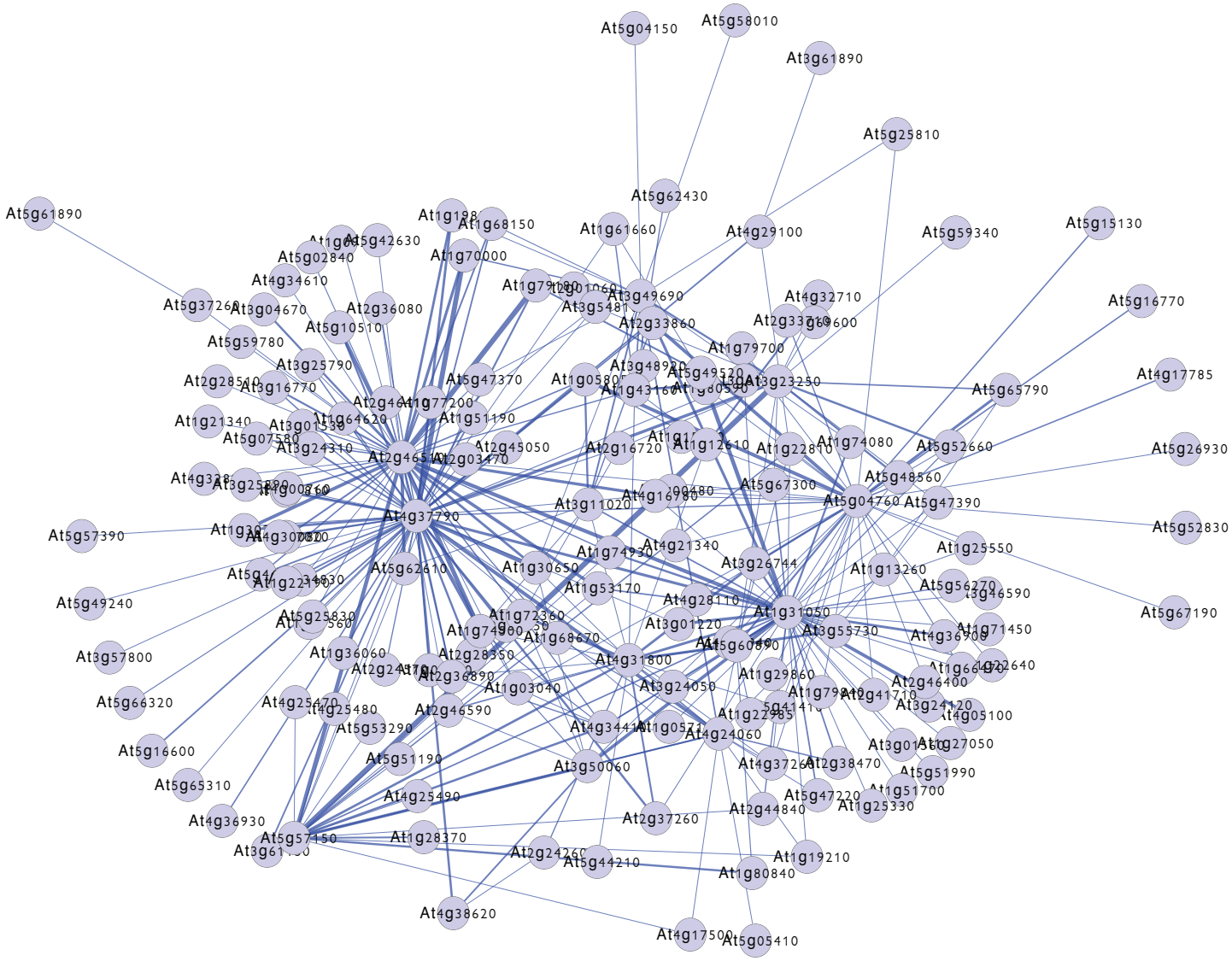

Figure 2. TransDetect network potentially influencing *PHO1;H3* gene expression. Each node represent a potential *PHO1;H3* regulator based on the TransDetect criteria defined in the text. If a pair of TF is predicted to explain *PHO1;H3* expression it is linked by an edge. The edge width is proportional to the sum of the R2 for the fit and predict processes (values are ranging from 16 to 176). The most influential factors are likely to be the most connected.

Figure 3

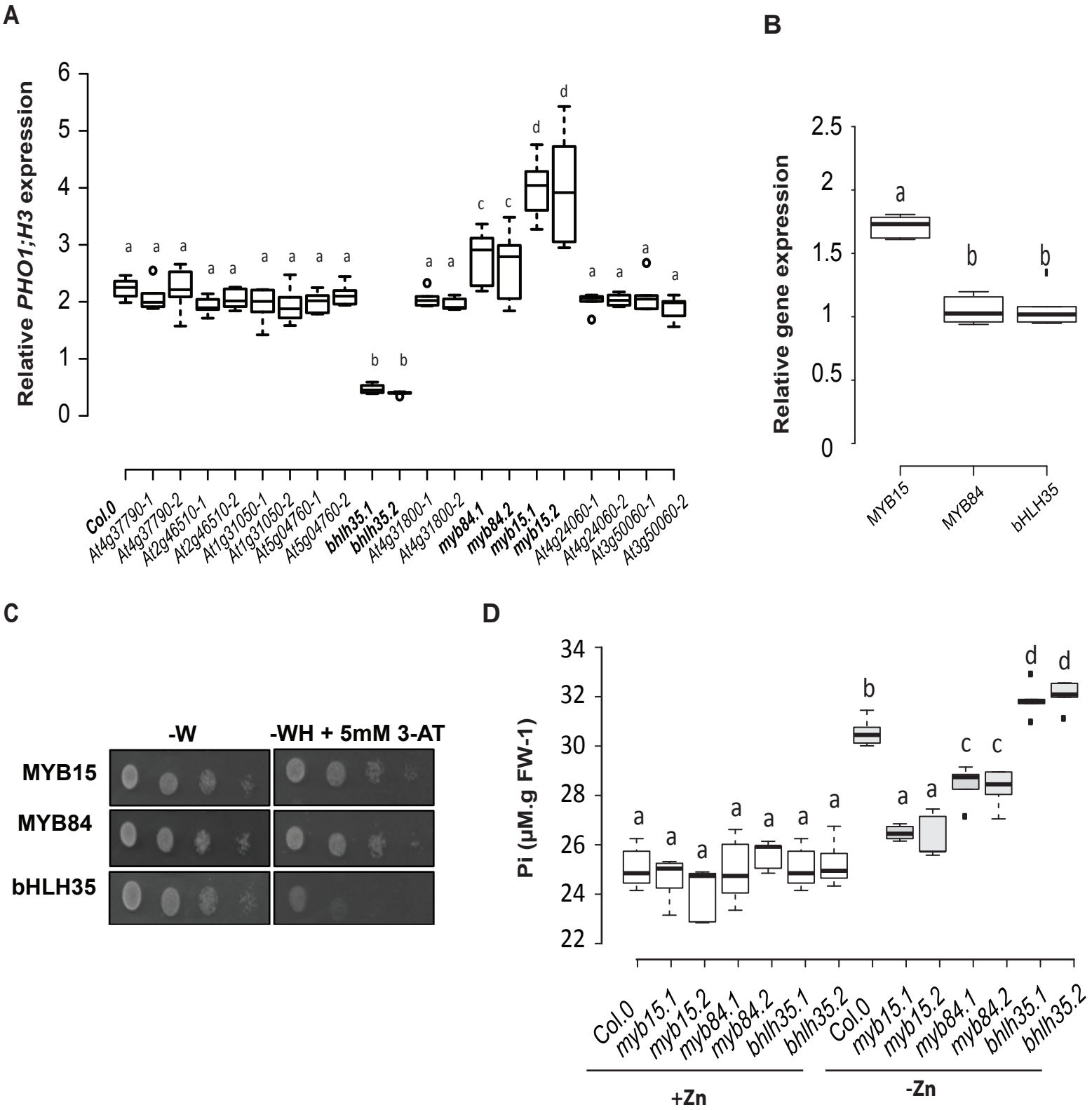

Figure 3. MYB15, MYB84 and bHLH35 regulate both the expression of *PHO1;H3* and the accumulation of Pi in the shoot under zinc deficiency. A- Relative *PHO1;H3* (At1g14040) transcript accumulation in the roots of wild-type plants (Col-0) and mutant lines harbouring loss-of-function mutations in the following transcription factors: At5g57150 (*bHLH35*), At3g23250 (*MYB15*), At3g49690 (*MYB84*), At4g37790 (*HAT22*), At2g46510 (*bHLH17*), At1g31050 (*bHLH111*), At5g04760 (*MYB*-type), At4g31800 (*WRKY18*), At4g24060 (*Dof46*) and At3g50060 (*MYB77*). Plants were grown for 18 days in the presence (+Zn) or absence (-Zn) of zinc. *PHO1;H3* transcript abundance was measured by qRT-PCR normalized against *UBQ10* (At4g05320). B- *MYB15*, *MYB84* and *bHLH35* transcripts accumulation in response to Zn deficiency. Relative *MYB15*, *MYB84* and *bHLH35* transcript accumulation was quantified in roots of wild-type plants (Col-0) grown for 18 days in the presence or absence of Zn by qRT-PCR and normalized against *UBQ10*. C- Yeast one-hybrid assay. Sequences of the Arabidopsis PHO1;H3 promoter fused to the HIS3 auxotrophic marker were stably transformed into yeast. These different yeast strains were then co-transfected with MYB15, MYB84 or bHLH35. Left panel, growth of the different yeast strains on control media deprived of tryptophan (-W), allowing the selection of yeast cells expressing the selected TFs. Right panel, growth of the different yeast strains on selective media deprived of tryptophan and histidine (-W -H). D- Pi concentrations measured in the shoots of wild type, *myb15*, *myb84*, or *bhlh35* plants grown for 18 days in the presence or absence of Zn. For A, C and D panels, central lines in the boxes show the medians; box limits indicate the 25th and 75th percentiles; whiskers extend 1.5 times the interquartile range from the 25th and 75th percentiles Letters a, b and c indicate significantly different values at p <005 determined by one-way ANOVA and Tukey HSD.

Figure 4

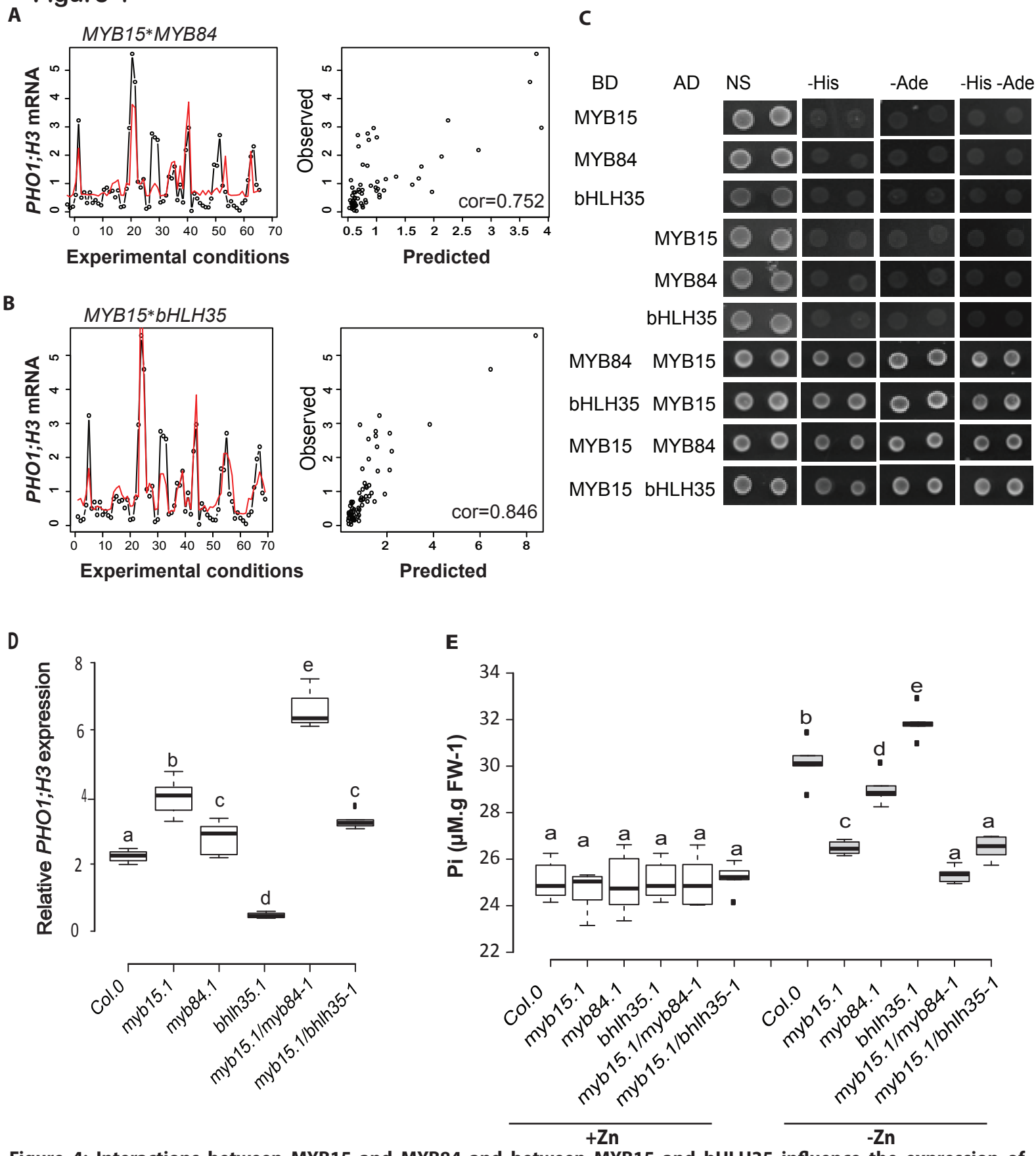

Figure 4: Interactions between MYB15 and MYB84 and between MYB15 and bHLH35 influence the expression of *PHO1;H3* and Pi accumulation under zinc deficiency. A, B- TransDetect's prediction of correlation between the expression of the MYB15 / MYB84 and MYB15 / bHLH35 TF pairs and the PHO1;H3 transcript level with R2=0.75 and R2=0.84 respectively. C- Yeast two-hybrid assay. bHLH35, MYB15 and MYB84 were fused with either the GAL4 DNA binding domain (BD) or the GAL4 activation domain (AD) into appropriate expression vectors, which were then transferred into yeast. The different yeast strains were plated on non-selective medium (NS) or on selective media deprived of histidine (-His), adenine (-Ade) or both simultaneously (-His-Ade). D- Relative *PHO1;H3* transcript accumulation in roots of wild type (Col-0), *bhlh35*, *myb15*, *myb84*, *myb15/myb84* and *myb15/bhlh35* single and double mutant plants grown for 18 days in the absence vs. presence of zinc (–Zn/+Zn). **PHO1;H3** transcript abundance was measured by qRT-PCR and normalized against *UBQ10*. E- Shoot Pi concentrations measured in wild-type (Col-0), bhlh35, myb15, myb84, myb15xmyb84 and myb15xbhlh35 single and double mutant plants grown on either +Zn or –Zn for 18 days. For D and E panels, Box central lines show the medians; box limits indicate the 25th and 75th percentiles; whiskers extend 1.5 times the interquartile range from the 25th and 75th percentiles. Letters a, b and c indicate significantly different values at p <0.05 determined by one-way ANOVA and Tukey HSD.

Figure 5

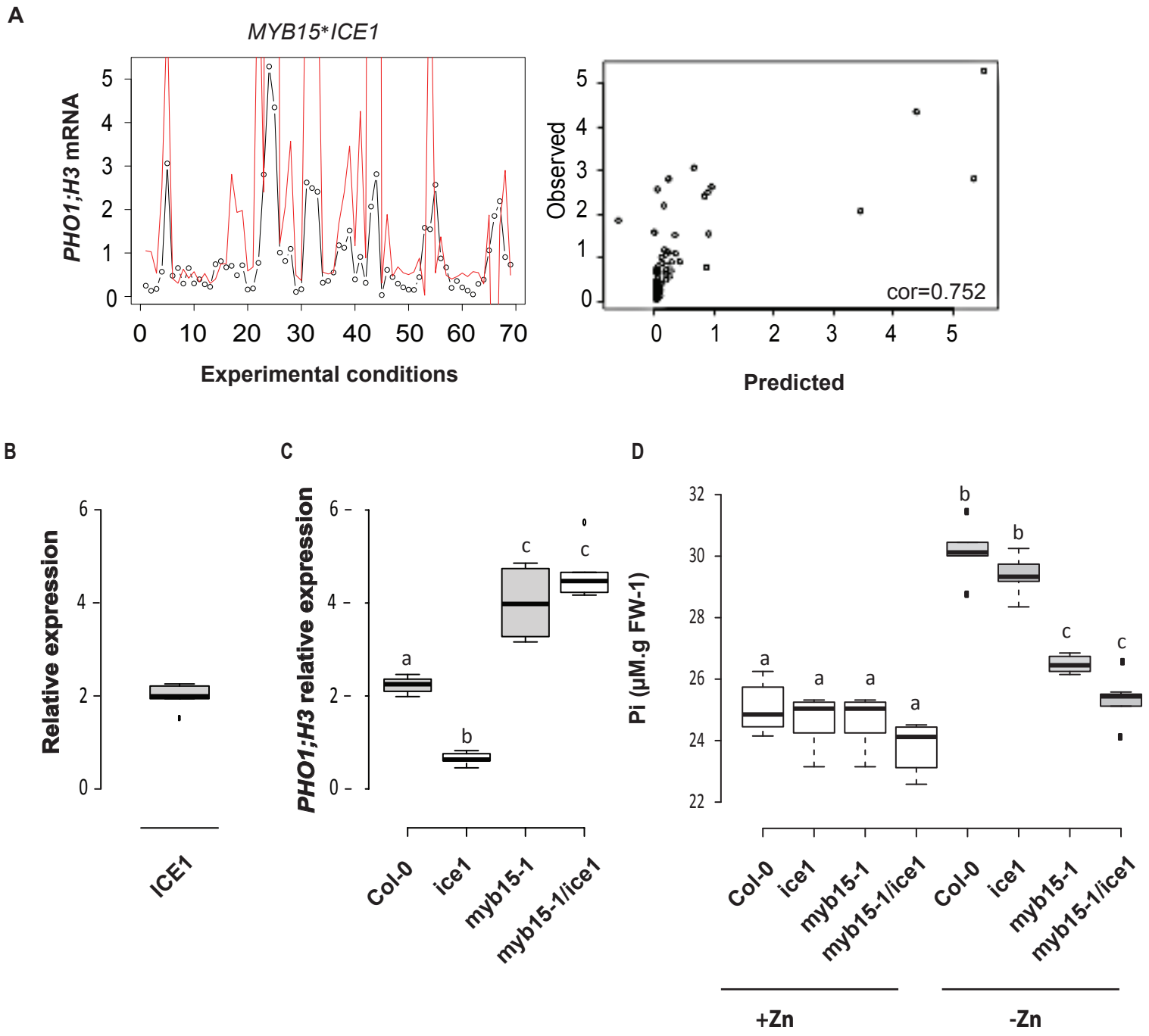

Figure 5. The ICE1 / MYB15 transcription factor pair regulates both the expression of *PHO1;H3* the accumulation Pi under –Zn. A- TransDetect's prediction of the correlation between the expression of the TF pair MYB15 and ICE1 and the *PHO1;H3* expression (R2=0,73). B- *ICE1* transcript accumulation. Expression of *ICE1* was quantified in wild-type (Col-0) seedlings grown for 18 days in presence (+Zn) or absence (-Zn) of zinc. *ICE1* transcript abundance was measured by qRT-PCR normalized against *UBQ10*. C- *PHO1;H3* transcript accumulation. Expression of *PHO1;H3* gene was quantified in wild type (Col-0), *ice1*, *myb15* and *myb15/ ice1* seedlings grown for 18 days in +Zn or –Zn. *PHO1;H3* transcript abundance was measured by qRT-PCR and normalized against *UBQ10*. D- Pi accumulations. Pi concentrations were measured from shoots of wild type (Col-0), ice1, myb15, and myb15 /ice1 seedlings grown for 18 days in presence +Zn or –Zn. For B, C and D, Box center lines show the medians; box limits indicate the 25th and 75th percentiles; whiskers extend 15 times the interquartile range from the 25th and 75th percentiles. Letters a, b and c indicate significantly different values at p<005 determined by one-way ANOVA and Tukey HSD.

Figure 6

A

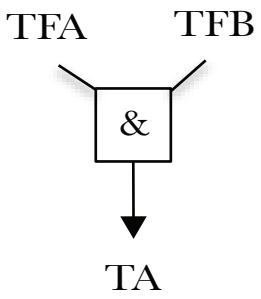

C

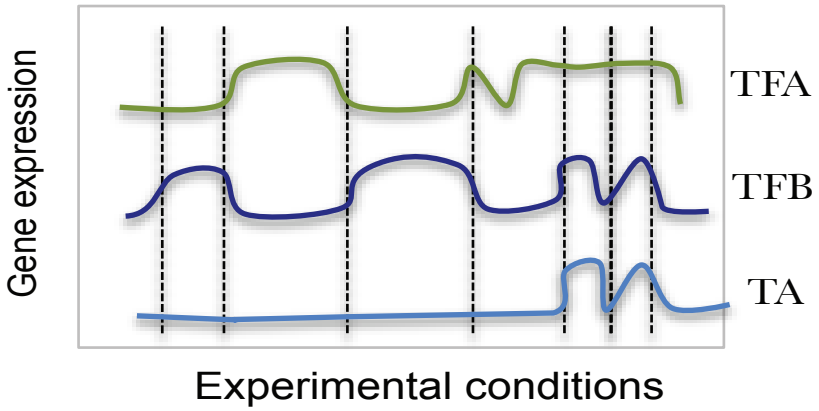

C

$$TA = \alpha TFA + \beta TFB + \gamma TFA*TFB + \varepsilon$$

Figure 6. Idealized model to explain how TransDetect extract directionality in static data. A- Two transcription factors TFA and TFB positively control the expression of a target gene TA following a AND logic-gate. B- TA expression is induced only when TFA and TFB expression are both upregulated. C- Linear modelling of TA expression. Considering the ideal case where 2 transcription factors (TFA and TFB) control a target gene TA following a AND logic gate. In this particular case, γ coefficient of the linear model will be highly significant because it is the combination of TFA and TFB expression that is necessary to fully explain TA expression. On the other hand it is not possible to infer TFA by a linear combination of TA and TFB, nor to explain TFB by a linear combination of TA and TFA. Thus the term of the equation γTFA*TFB intrinsically possess some directionality explanatory power in this case where both TFs interact in the control of TA.

Figure 7

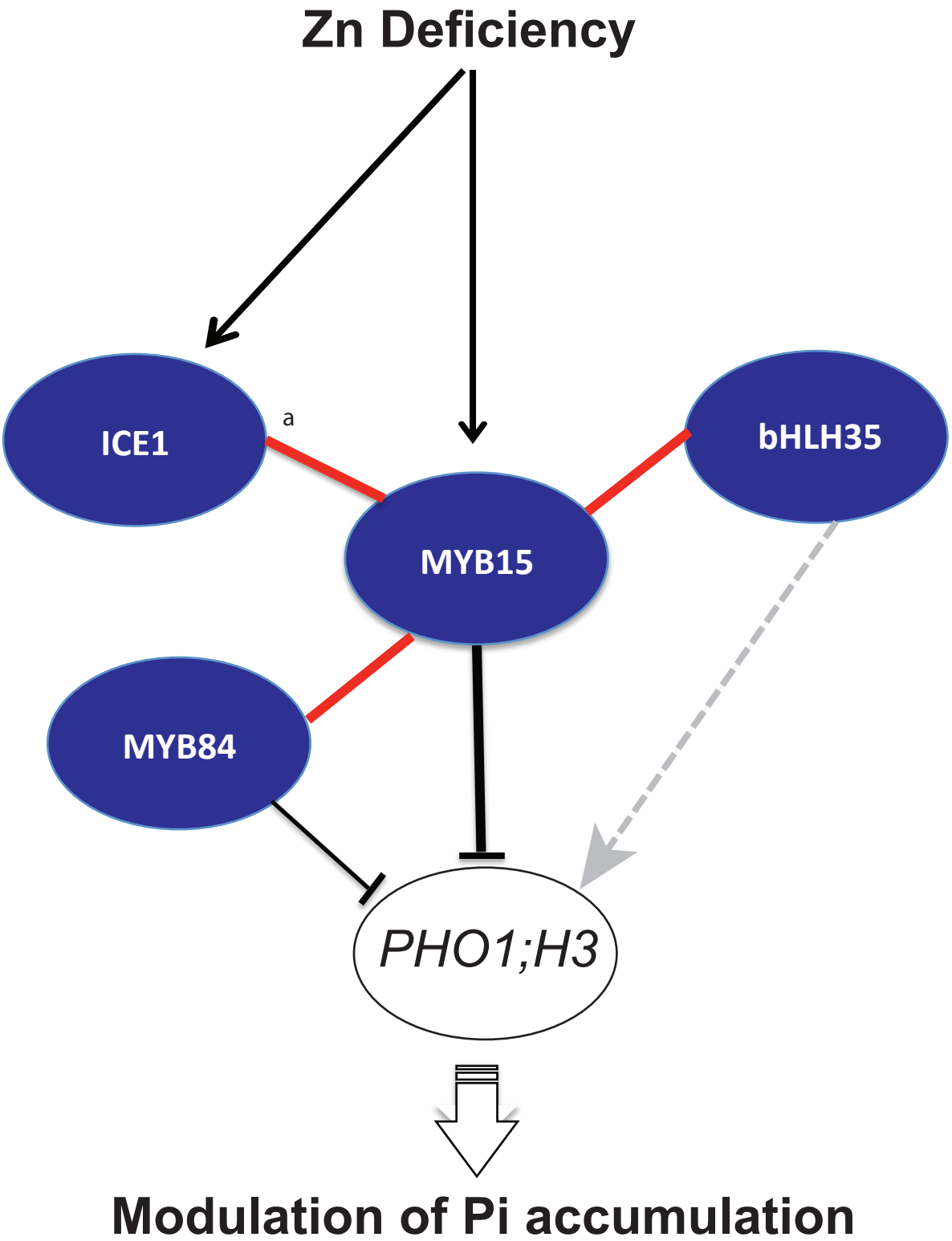

Figure 7. Schematic representation of the MYB15, MYB84, bHLH35 and ICE1 regulatory module controlling *PHO1;H3* gene expression and Pi accumulation in shoots under zinc deficiency. Phosphate increases in the shoots of plants exposed to zinc deficiency. PHO1;H3 plays a negative regulatory role in this process. Red solid lines indicate connections between MYB15, MYB84, bHLH35 and ICE1. Negative and positive regulatory effects of these transcription factors on PHO1;H3 expression under zinc deficiency are indicated by flat-ended dashed lines and arrowheads, respectively. a indicates previous knowledge on ICEI and MYB15 physical interaction.

Supplementray Figure 1

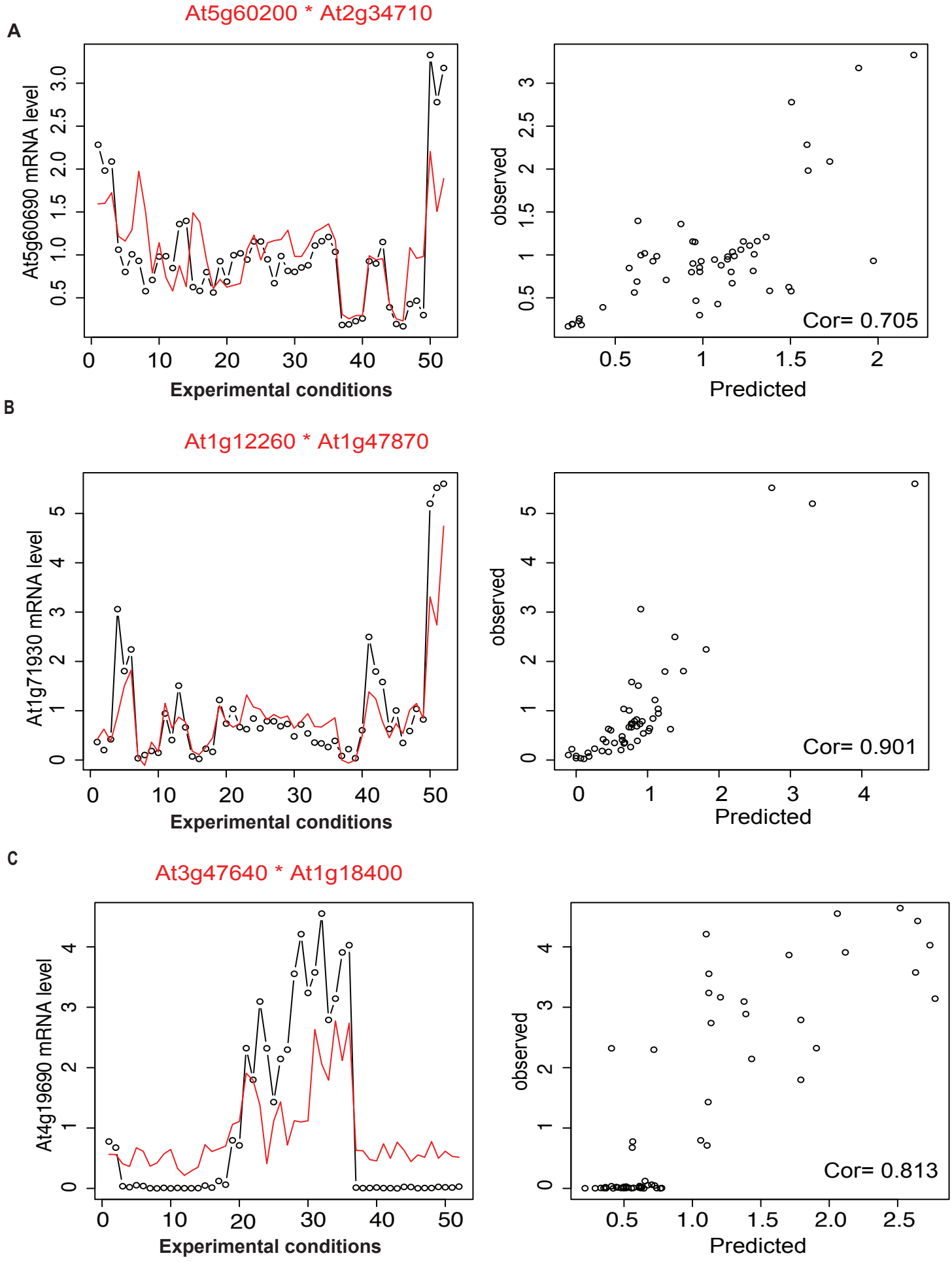

Supplementary Figure 1. TransDetect prediction of regulators for *REVOLUTA*, *ASCULAR RELATED NAC-DOMAIN PROTEIN 7* and *IRON-REGULATED TRANSPORTER 1*. TransDetect was used to predict regulators for the following target genes A- *REVOLUTA* (*REV*, At5g60690), B- *ASCULAR RELATED NAC-DOMAIN PROTEIN 7* (*VND7*, At1g71930), and C- *IRON-REGULATED TRANSPORTER 1* (*IRT1*, At4g19690). Among number of TFs predicted, TransDetect retrieved known regulators for theses genes, namely DNA BINDING WITH ONE FINGER 5.3 (DOF5.3, At5g60200) for *REV*, ARABIDOPSIS THALIANA HOMOLOG OF E2F C TF (E2Fc, At1g47870) for *VND7*, and POPEYE (PYE, At3g47640) for *IRT1*.

Parsed Citations

Agarwal M, Hao Y, Kapoor A, Dong C-H, Fujii H, Zheng X, Zhu, J-K (2006) A R2R3 type MYB transcription factor is involved in the cold regulation of CBF genes in acquired freezing tolerance. J Biol Chem 281: 37636-37645

Pubmed: Author and Title
CrossRef: Author and Title
Google Scholar: Author Only Title Only Author and Title

Alonso JM, Stepanova AN, Leisse TJ, Kim CJ, Chen H, Shinn P, Stevenson DK, Zimmerman J, Barajas P, Cheuk R (2003) Genome-wide insertional mutagenesis of Arabidopsis thaliana. Science 301:653-657

Pubmed: Author and Title
CrossRef: Author and Title
Google Scholar: Author Only Title Only Author and Title

Ames BN (1966) Assay of inorganic phosphate, total phosphate and phosphatases. Methods Enzymol. 8: 115-118

Pubmed: Author and Title
CrossRef: Author and Title
Google Scholar: Author Only Title Only Author and Title

Assunção AG, Herrero E, Lin Y-F, Huettel B, Talukdar S, Smaczniak C, Immink RG, Van Eldik M, Fiers M, Schat H (2010) Arabidopsis thaliana transcription factors bZIP19 and bZIP23 regulate the adaptation to zinc deficiency Proc Natl Acad Sci 107: 10296-10301

Pubmed: Author and Title
CrossRef: Author and Title
Google Scholar: Author Only Title Only Author and Title

Azevedo H, Azinheiro SG, Muñoz-Mérida A, Castro PH, Huettel B, Aarts MM, Assunção AG (2016) Transcriptomic profiling of Arabidopsis gene expression in response to varying micronutrient zinc supply. Genom data 7: 256-258

Pubmed: Author and Title
CrossRef: Author and Title
Google Scholar: Author Only Title Only Author and Title

Bargmann BO, Marshall-Colon A, Efroni I, Ruffel S, Birnbaum KD, Coruzzi GM, Krouk G (2013) TARGET: a transient transformation system for genome-wide transcription factor target discovery. Mol Plant 6: 978-980

Pubmed: Author and Title
CrossRef: Author and Title
Google Scholar: Author Only Title Only Author and Title

Bari R, Pant BD, Stitt M, Scheible W-R (2006) PHO2, microRNA399, PHR1 define a phosphate-signaling pathway in plants. Plant Physiol: 141. 988-999

Pubmed: Author and Title
CrossRef: Author and Title
Google Scholar: Author Only Title Only Author and Title

Bouain N, Shahzad Z, Rouached A, Khan GA, Berthomieu P, Abdelly C, Poirier Y, Rouached H (2014) Phosphate and zinc transport and signalling in plants: toward a better understanding of their homeostasis interaction. J Exp Bot 65: 5725-5741

Pubmed: Author and Title
CrossRef: Author and Title
Google Scholar: Author Only Title Only Author and Title

Brady SM, Orlo DA, Lee J-Y, Wang JY, Koch J, Dinneny JR, Mace D, Ohler U, Benfey PN (2007) A high-resolution root spatiotemporal map reveals dominant expression patterns. Science 318: 801-806

Pubmed: Author and Title
CrossRef: Author and Title
Google Scholar: Author Only Title Only Author and Title

Brady SM, Zhang L, Megraw M, Martinez NJ, Jiang E, Charles SY, Liu W, Zeng A, Taylor-Teeples M, Kim D (2011) A stele-enriched gene regulatory network in the Arabidopsis root. Mol Syst Biol 7: 459

Pubmed: Author and Title
CrossRef: Author and Title
Google Scholar: Author Only Title Only Author and Title

Chang Y-H, Wang Y-C, Chen B-S (2006) Identification of transcription factor cooperativity via stochastic system model. Bioinformatics 22: 2276-2282

Pubmed: Author and Title
CrossRef: Author and Title
Google Scholar: Author Only Title Only Author and Title

Datta D, Zhao H (2008) Statistical methods to infer cooperative binding among transcription factors in Saccharomyces cerevisiae. Bioinformatics 24: 545-552

Pubmed: Author and Title
CrossRef: Author and Title
Google Scholar: Author Only Title Only Author and Title

Denay G, Creff A, Moussu S, Wagnon P, Thévenin J, Gérentes M-F, Chambrier P, Dubreucq B, Ingram, G (2014) Endosperm breakdown

in Arabidopsis requires heterodimers of the basic helix-loop-helix proteins ZHOUPI INDUCER OF CBP EXPRESSION 1. Development 141: 1222-1227
Pubmed: Author and Title
CrossRef: Author and Title
Google Scholar: Author Only Title Only Author and Title

Dinneny JR, Long TA, Wang JY, Jung JW, Mace D, Pointer S, Barron C, Brady SM, Schiefelbein J, Benfey PN (2008) Cell identity mediates the response of Arabidopsis roots to abiotic stress. Science 320: 942-945
Pubmed: Author and Title
CrossRef: Author and Title
Google Scholar: Author Only Title Only Author and Title

Doidy J, Li Y, Neymotin B, Edwards MB, Varala K, Gresham D, Coruzzi GM (2016) Hit-and-Run" transcription: de novo transcription initiated by a transient bZIP1 "hit" persists after the "run". BMC genomics 17: 1
Pubmed: Author and Title
CrossRef: Author and Title
Google Scholar: Author Only Title Only Author and Title

Dubos C, Kelemen Z, Sebastian A, Bülow L, Huep G, Xu W, Grain D, Salsac F, Brousse C, Lepiniec, L (2014) Integrating bioinformatic resources to predict transcription factors interacting with cis-sequences conserved in co-regulated genes. BMC genomics 15: 1
Pubmed: Author and Title
CrossRef: Author and Title
Google Scholar: Author Only Title Only Author and Title

Gaudinier A, Zhang L, Reece-Hoyes JS, Taylor-Teeples M, Pu L, Liu Z, Breton G, Pruneda-Paz, JL, Kim D, Kay SA (2011) Enhanced Y1H assays for Arabidopsis. Nature methods 8: 1053-1055
Pubmed: Author and Title
CrossRef: Author and Title
Google Scholar: Author Only Title Only Author and Title

GuhaThakurta D, Stormo GD (2001) Identifying target sites for cooperatively binding factors. Bioinformatics 17: 608-621
Pubmed: Author and Title
CrossRef: Author and Title
Google Scholar: Author Only Title Only Author and Title

Jain A, Nagarajan VK, Raghothama KG (2012) Transcriptional regulation of phosphate acquisition by higher plants. Cell Mol Life Sci 69: 3207-3224
Pubmed: Author and Title
CrossRef: Author and Title
Google Scholar: Author Only Title Only Author and Title

Katari MS, Nowicki SD, Aceituno FF, Nero D, Kelfer J, Thompson LP, Cabello JM, Davidson RS, Goldberg AP, Shasha DE (2010) VirtualPlant: a software platform to support systems biology research. Plant Physiol 152: 500-515
Pubmed: Author and Title
CrossRef: Author and Title
Google Scholar: Author Only Title Only Author and Title

Kaufmann K, Pajoro A, Angenent GC (2010a) Regulation of transcription in plants: mechanisms controlling developmental switches. Nat Rev Genet 11: 830-842
Pubmed: Author and Title
CrossRef: Author and Title
Google Scholar: Author Only Title Only Author and Title

Kaufmann K, Muino JM, Østerås M, Farinelli L, Krajewski P, Angenent GC (2010b) Chromatin immunoprecipitation (ChIP) of plant transcription factors followed by sequencing (ChIP-SEQ) or hybridization to whole genome arrays (ChIP-CHIP). Nature Protocols 5: 457-472
Pubmed: Author and Title
CrossRef: Author and Title
Google Scholar: Author Only Title Only Author and Title

Kelemen Z, Sebastian A, Xu W, Grain D, Salsac F, Avon A, Berger N, Tran J, Dubreucq B, Lurin C (2015) Analysis of the DNA-Binding Activities of the Arabidopsis R2R3-MYB Transcription Factor Family by One-Hybrid Experiments in Yeast. PloS One 10: e0141044
Pubmed: Author and Title
CrossRef: Author and Title
Google Scholar: Author Only Title Only Author and Title

Khan GA, Bouraine S, Wege S, Li Y, De Carbonnel M, Berthomieu P, Poirier Y, Rouached H (2014) Coordination between zinc and phosphate homeostasis involves the transcription factor PHR1, the phosphate exporter PHO1, its homologue PHO1; H3 in Arabidopsis. J Exp Bot 65: 871-884
Pubmed: Author and Title
CrossRef: Author and Title
Google Scholar: Author Only Title Only Author and Title

Krouk G, Lingeman J, Colon AM, Coruzzi G, Shasha D (2013) Gene regulatory networks in plants: learning causality from time perturbation. Genome biol 14: 1

Pubmed: Author and Title
CrossRef: Author and Title
Google Scholar: Author Only Title Only Author and Title

Lin S-I, Chiang S-F, Lin W-Y, Chen J-W, Tseng C-Y, Wu P-C, Chiou T-J (2008) Regulatory network of microRNA399 and PHO2 by systemic signalling. Plant Physiol 147: 732-746
Pubmed: Author and Title
CrossRef: Author and Title
Google Scholar: Author Only Title Only Author and Title

Livak KJ, Schmittgen TD (2001) Analysis of relative gene expression data using real-time quantitative PCR the 2- ??CT method. Methods 25: 402-408
Pubmed: Author and Title
CrossRef: Author and Title
Google Scholar: Author Only Title Only Author and Title

Long TA, Tsukagoshi H, Busch W, Lahner B, Salt DE, Benfey PN (2010) The bHLH transcription factor POPEYE regulates response to iron deficiency in Arabidopsis roots. Plant Cell 22: 2219-2236
Pubmed: Author and Title
CrossRef: Author and Title
Google Scholar: Author Only Title Only Author and Title

Medici A, Marshall-Colon A, Ronzier E, Szponarski W, Wang R, Gojon A, Crawford NM, Ruffel S, Coruzzi GM, Krouk G (2015) AtNIGT1/HRS1 integrates nitrate and phosphate signals at the Arabidopsis root tip. Nat Commun 6: 6274
Pubmed: Author and Title
CrossRef: Author and Title
Google Scholar: Author Only Title Only Author and Title

Miura K, Jin JB, Lee J, Yoo CY, Stirm V, Miura T, Ashworth EN, Bressan RA, Yun D-J, Hasegawa PM (2007) SIZ1-mediated sumoylation of ICE1 controls CBF3/DREB1A expression freezing tolerance in Arabidopsis. Plant Cell 19: 1403-1414
Pubmed: Author and Title
CrossRef: Author and Title
Google Scholar: Author Only Title Only Author and Title

Mongon J, Chaiwong N, Bouain N, Prom-u-Thai C, Secco D, Rouached H (2017) Phosphorus and iron deficiencies influences Rice Shoot Growth in an Oxygen Dependent Manner: Insight from Upl Lowl rice. IJMS 18: 607
Pubmed: Author and Title
CrossRef: Author and Title
Google Scholar: Author Only Title Only Author and Title

Nagamine N, Kawada Y, Sakakibara Y (2005) Identifying cooperative transcriptional regulations using protein-protein interactions. Nucleic Acids Res 33: 4828-4837
Pubmed: Author and Title
CrossRef: Author and Title
Google Scholar: Author Only Title Only Author and Title

Nagel DH, Doherty CJ, Pruneda-Paz JL, Schmitz RJ, Ecker JR, Kay SA (2015) Genome-wide identification of CCA1 targets uncovers an exped clock network in Arabidopsis. Proc Natl Acad Sci 112: E4802-E4810
Pubmed: Author and Title
CrossRef: Author and Title
Google Scholar: Author Only Title Only Author and Title

O'Malley RC, Huang S-sC, Song L, Lewsey MG, Bartlett A, Nery JR, Galli M, Gallavotti A, Ecker JR (2016) Cistrome Epicistrome Features Shape the Regulatory DNA Lscape. Cell 165: 1280-1292
Pubmed: Author and Title
CrossRef: Author and Title
Google Scholar: Author Only Title Only Author and Title

Para A, Li Y, Marshall-Colón A, Varala K, Francoeur NJ, Moran TM, Edwards MB, Hackley C, Bargmann BO, Birnbaum KD (2014) Hit--run transcriptional control by bZIP1 mediates rapid nutrient signaling in Arabidopsis. Proc Natl Acad Sci 111: 10371-10376
Pubmed: Author and Title
CrossRef: Author and Title
Google Scholar: Author Only Title Only Author and Title

Qin J, Hu Y, Xu F, Yalamanchili HK, Wang J (2014) Inferring gene regulatory networks by integrating ChIP-seq/chip transcriptome data via LASSO-type regularization methods. Methods 67: 294-303
Pubmed: Author and Title
CrossRef: Author and Title
Google Scholar: Author Only Title Only Author and Title

Riechmann, JL, Heard, J, Martin, G, Reuber, L, Jiang, C, Keddie, J, Adam, L, Pineda, O, Ratcliffe OJ, Samaha RR, Creelman R, Pilgrim M, Broun P, Zhang JZ, Ghehari D, Sherman BK, Yu G (2000) Arabidopsis transcription factors: genome-wide comparative analysis among eukaryotes. Science 290: 2105-2110
Pubmed: Author and Title
CrossRef: Author and Title
Google Scholar: Author Only Title Only Author and Title

Rouached H, Rhee SY (2017) System-level understanding of plant mineral nutrition in the big data era.

Curr Opin Syst Biol. 4: 71-77

Rouached H, Stefanovic A, Secco D, Bulak Arpat A, Gout E, Bligny R, Poirier Y (2011) Uncoupling phosphate deficiency from its major effects on growth transcriptome via PHO1 expression in Arabidopsis. Plant J 65: 557-570

Pubmed: Author and Title
CrossRef: Author and Title
Google Scholar: Author Only Title Only Author and Title

Rouached H, Wirtz M, Alary R, Hell R, Arpat AB, Davidian J-C, Fourcroy P, Berthomieu P (2008) Differential regulation of the expression of two high-affinity sulfate transporters, SULTR1 ;1 and SULTR1 ;2, in Arabidopsis. Plant Physiol 147: 897-911

Pubmed: Author and Title
CrossRef: Author and Title
Google Scholar: Author Only Title Only Author and Title

Taylor-Teeples M, Lin L, de Lucas M, Turco G, Toal T, Gaudinier A, Young N, Trabucco G, Veling M, Lamothe R (2015) An Arabidopsis gene regulatory network for secondary cell wall synthesis. Nature 517: 571-575

Pubmed: Author and Title
CrossRef: Author and Title
Google Scholar: Author Only Title Only Author and Title

Xu W, Grain D, Gourrierec J, Harscoët E, Berger A, Jauvion V, Scagnelli A, Berger N, Bidzinski P, Kelemen Z (2013) Regulation of flavonoid biosynthesis involves an unexpected complex transcriptional regulation of TT8 expression, in Arabidopsis. New Phytol 198: 59-70

Pubmed: Author and Title
CrossRef: Author and Title
Google Scholar: Author Only Title Only Author and Title

Yu X, Lin J, Zack DJ, Qian J (2006) Computational analysis of tissue-specific combinatorial gene regulation: predicting interaction between transcription factors in human tissues. Nucleic Acids Res 34: 4925-4936

Pubmed: Author and Title
CrossRef: Author and Title
Google Scholar: Author Only Title Only Author and Title